Article

Not peer-reviewed version

Highly Sensitive and Specific Detection of Influenza A Viruses Using Bimolecular Fluorescence Complementation (BiFC) Reporter System

Ui Jin Lee , Yunkwang Oh , Oh Seok Kwon , Yong-Beom Shin , Moonil Kim *

Posted Date: 29 June 2023

doi: 10.20944/preprints202306.2151.v1

Keywords: bimolecular fluorescence complementation; BiFC; influenza A virus; IAV; biosensor

Article

Highly Sensitive and Specific Detection of Influenza A Viruses Using Bimolecular Fluorescence Complementation (BiFC) Reporter System

Ui Jin Lee [1,*], Yunkwang Oh [1,*], Oh Seok Kwon [2,3,4], Yong-Beom Shin [5,6,7] and Moonil Kim [1,5,7,†]

1 Critical Diseases Diagnostics Convergence Research Center, Korea Research Institute of Bioscience and Biotechnology (KRIBB), 125 Gwahang-ro, Yuseong-gu, Daejeon 34141, Republic of Korea; waainie@eyebiokorea.com (U.J.L.); oyk0213@kribb.re.kr (Y.O.)
2 SKKU Advanced Institute of Nanotechnology (SAINT), Sungkyunkwan University, Suwon 16419, Republic of Korea; oskwon79@skku.edu (O.S.K.)
3 Department of Nano Science and Technology, Sungkyunkwan University, Suwon 16419, Republic of Korea
4 Department of Nano Engineering, Sungkyunkwan University, Suwon 16419, Republic of Korea
5 Bionanotechnology Research Center, Korea Research Institute of Bioscience and Biotechnology (KRIBB), Daejeon 34141, Republic of Korea; ybshin@kribb.re.kr (Y.B.S.)
6 BioNano Health Guard Research Center (H-GUARD), Daejeon 34141, Republic of Korea
7 KRIBB School, Korea University of Science and Technology (UST), 217 Gajeong-ro, Yuseong-gu, Daejeon 34113, Republic of Korea
* These authors contributed equally to this work.
† Correspondence: kimm@kribb.re.kr (M.K.); Tel.: +82-42-8798447; Fax: +82-42-879-8594

Abstract: Herein, we developed a highly sensitive and specific bimolecular fluorescence complementation (BiFC)-based influenza A virus (IAV) sensing system created by combining a galactose/glucose-binding protein (GGBP) with an N-terminal large domain (YN1-172) and a C-terminal small domain (YC173-239) of enhanced yellow fluorescence protein (eYFP). The GGBP-based BiFC reporter exhibits the fluorescence reconstitution as a result of conformational changes in GGBP when lactose, derived from 6′-silalyllactose used as a substrate for neuraminidase (NA), binds to GGBP in the presence of IAV. The system showed a linear dynamic range from 1 x 10^0 $TCID_{50}$/mL to 1 x 10^7 $TCID_{50}$/mL, with a detection limit of 4 x 10^1 $TCID_{50}$/mL for IAV (H1N1), demonstrating ultra-high sensitivity. Our system exhibited fluorescence intensity enhancements in the presence of IAV, while displaying weak fluorescence signals when exposed to NA-deficient viruses such as RSV A, RSV B, adenovirus and rhinovirus, thereby indicating selective responses for IAV detection. Taken together, our system provides a simple, highly sensitive and specific IAV detection platform based on BiFC capable of detecting the ligand-induced protein conformational changes, obviating the need for virus culture or RNA extraction processes.

Keywords: bimolecular fluorescence complementation; BiFC; influenza A virus; IAV; biosensor

1. Introduction

Influenza A virus (IAV) is the predominant type responsible for most cases of influenza, and it annually causes widespread outbreaks worldwide [1,2]. The influenza virus encompasses diverse lineages that contribute to the periodic occurrence of seasonal influenza. As an example, the H1N1 lineage was the causative agent of the global pandemic that occurred from 2009 to 2010 [3,4]. Neuraminidase (NA), one of the major surface proteins of IAV, plays a crucial role in the release of nascent viral particles assembled in infected cells. It facilitates the discharge of these particles from cells by cleaving sialic acid residues found in the glycan component attached to glycoproteins on the cell's plasma membrane [5–7].

The diagnosis of human IAV infections is typically achieved through viral culture, molecular-based diagnosis tests and immunological diagnostic approaches [8–11]. In conventional practice, the measurement of virus infectivity involves conducting the plaque assay or focus assay in cell cultures

 doi:10.20944/preprints202306.2151.v1

[12,13]. These methods continue to be widely used for assessing virus infectivity due to their reliability. Nevertheless, they require several days to obtain results and proper handling of the organism [14]. Molecular-based diagnosis tests encompass techniques such as reverse transcription PCR (RT-PCR), real-time PCR and isothermal amplification methods. PCR has the advantage of high sensitivity to detect low virus quantities during the early stages of infection. However, it requires specialized equipment, trained personnel and may not provide rapid results [15,16]. Isothermal amplification methods like nucleic acid sequence-based amplification (NASBA), loop-mediated isothermal amplification (LAMP), recombinase polymerase amplification (RPA) and so on offer relatively fast and sensitive reaction, becoming the next gold standard amplification techniques. Despite the advantages of isothermal reaction, the low temperature between 30°C and 55°C makes it prone to unspecific primer-binding that might cause unspecific amplifications [17,18]. Immunological diagnostic approaches such as enzyme-linked immunosorbent assay (ELISA), immunofluorescence assay (IFA) and rapid influenza diagnostic test (RIDT) are widely used for IAV detection [19–21]. These methods, along with standardized protocols and commercial kits, enable rapid detection of IAV in laboratory and field settings. However, they have lower sensitivity compared to molecular diagnostics and may exhibit cross-reactivity with other viral antigens [22].

Bimolecular fluorescence complementation (BiFC) system involves expressing fluorescence proteins as two fragments, which do not produce fluorescence when far apart, but restore fluorescence when brought close together [23–25]. The system has been widely regarded as a potent tool that utilizes a split reporter strategy to analyze protein conformational changes as well as protein-protein interactions in various cell types and organisms [26,27]. In this study, we developed an IAV sensing system designed by combining a GGBP with a BiFC reporter protein, and using 6′-sialyllactose as a substrate. The designed molecular system utilizes a split eYFP as a transducer to convert the structural changes of GGBP into fluorescence. The underlying principle of the GGBP-based BiFC reporter system relies on the fluorescence reconstitution triggered by the conformational changes of GGBP upon the binding of lactose, which is cleaved from 6′-sialyllactose, to GGBP in the presence of IAV. Our system demonstrated outstanding sensitivity, wide dynamic range and specificity towards IAV. Particularly, the achieved detection limit of 4 x 10^1 $TCID_{50}$/mL for IAV (H1N1) obtained from the current study demonstrates the potential applicability of our system in on-site testing or primary screening where highly sensitive and direct detection without virus amplification is required.

2. Materials and Methods

2.1. Materials, strains, vectors and enzymes

Glucose, galactose and lactose were purchased from Sigma-Aldrich (St. Louis, MO), and 6′-sialyllactose was obtained from Biosynth (UK). Oseltamivir carboxylate, the active form of oseltamivir, was obtained from Adamas Pharmaceuticals (Emeryville, CA). E. coli strian DH5α was used as host for subcloning and E. coli BL21 (DE3) (Novagen, WI) for gene expression. pGEM-T (Promega, WI) and pET-21a(+) (Novagen, WI) were used as vectors for subcloning and protein expression, respectively. All the restriction enzymes and modifying enzymes were purchased from Nanohelix (Korea), and used according to the recommendations of supplier. A preparation of vector DNA was carried out using QIAEX II gel extraction kit (Qiagen, Germany).

2.2. Viruses

Influenza A viruses (H1N1, H1N2, H3N8 and H6N5) suspended in cell culture medium (MEM, MDCK cells) were obtained from the BioNano Health Guard Research Center (H-GUARD). Respiratory syncytial virus (RSV), adenovirus and rhinovirus were provided by the Korea Bank for Pathogenic Viruses (KBPV).

2.3. Reporter plasmid construction

 doi:10.20944/preprints202306.2151.v1

The cloning of the YN1YC173 construct was achieved using the multiple fragment assembly method. For the YN1-172-linker-1 fragment, the partial gene encompassing amino acids 1-172 of eYFP was amplified with the corresponding primers (forward primer: 5′-CAT ATG GTG AGC AAG GGC GAG GAG-3′/ reverse primer: 5′-GGA TCC CAT ATG TGA TGA GGT ACC GAT GTT GTG GCG GAT CTT-3′), ensuring the inclusion of the linker-1 sequence (GTSSHM) and specific restriction enzyme cleavage sites (NdeI and BamHI) at the 5' and 3' termini. Similarly, the GGBP1-32-linker-2 fragment involved amplification of the gene segment encoding amino acids 1-32 of GGBP, with appropriate primers (forward primer: 5′-GGA TCC GCT GAT ACT CGC ATT GGT-3′/ reverse primer: 5′-GTC GAC TGA ACC TGA ACC GGT ACC TGG CGC GGC TTT CGC ATC-3′) designed to incorporate the linker-2 sequence (GTGSGS) and desired restriction enzyme cleavage sites (BamHI and SalI). For the YC173-239-linker-3 fragment, the partial gene encoding amino acids 173-239 of eYFP was PCR-amplified using specific primers (forward primer: 5′-GTC GAC GAG GAC GGC AGC GTG CAG-3′/ reverse primer: 5′-AAG CTT CAT ATG ACC TGA ACC CTT GTA CAG CTC GTC CAT-3′), also designed to include the linker-3 sequence (GSGHM) and desired restriction enzyme cleavage sites (SalI and HindIII). Finally, the GGBP33-309 fragment was generated by amplifying the partial gene encoding amino acids 33-309 of GGBP, utilizing the designated primers (forward primer: 5′-AAG CTT GAT GTT CAG CTG CTG ATG-3′/ reverse primer: 5′-CTC GAG TTT CTT GCT GAA TTC AGC-3′) incorporating the specified restriction enzyme cleavage sites (HindIII and XhoI) at the termini. The plasmid construct design involved combining incompatible-ended fragments and a linearized vector, resulting in the successful construction of the YN1YC173 construct. This was achieved by mixing the four PCR fragments (YN1-172-linker-1, GGBP1-32-linker-2, YC173-239-linker-3 and GGBP33-309) with the linearized vector (pET-21a(+)), cleaved by the indicated restriction enzymes, in a single ligation reaction. The cloning of the YN1YC155 construct was carried out using the same multiple fragment assembly procedure as in the YN1YC173 consturct. For the YN1-154-linker-1 fragment, the gene segment encoding amino acids 1-154 of eYFP was amplified through PCR using the corresponding primers (forward primer: 5′-CAT ATG GTG AGC AAG GGC GAG GAG-3′/ reverse primer: 5′-GGA TCC CAT ATG TGA TGA GGT ACC CAT GAT ATA GAC GTT GTG-3′), designed to include the linker-1 sequence (GTSSHM) and desired restriction enzyme cleavage sites (NdeI and BamHI). For the YC155-239-linker-3 fragment, the partial gene encompassing amino acids 155-239 of eYFP was PCR-amplified using the designated primers (forward primer: 5′- GTC GAC GCC GAC AAG CAG AAG AAC-3′/ reverse primer: 5′- AAG CTT CAT ATG ACC TGA ACC CTT GTA CAG CTC GTC CAT-3′) incorporating the linker-3 sequence (GSGHM) and the specified restriction enzyme cleavage sites (SalI and HindIII) at the termini. By combining the four PCR fragments (YN1-154-linker-1, GGBP1-32-linker-2, YC155-239-linker-3 and GGBP33-309) with the linearized vector (pET-21a(+)) cleaved by the indicated restriction enzymes, a single ligation reaction was performed, leading to the successful assembly of the YN1YC155 construct. The choice of flexible linkers was based on a previous report highlighting the flexibility conferred by these small amino acids, enabling the mobility of the connected functional domains [28].

2.4. Site-directed mutagenesis

For the cloning of the mutant YN1YC173-Asp14Ile, overlap extension PCR-based site-directed mutagenesis was conducted with flanking primers (forward primer: 5′-CAT ATG GTG AGC AAG GGC GAG GAG-3′/ reverse primer: 5′- CTC GAG TTT CTT GCT GAA TTC AGC-3′) on both ends of the template and internal primers (forward primer: 5′-TAT AAG TAC GAC ATC AAC TTT ATG TCT-3′/ reverse primer: 5′-AGA CAT AAA GTT GAT GTC GTA CTT ATA-3′) that contain the base changes of interest and bind to the region where the replacement will occur. The resulting PCR products were then inserted into the pET-21a(+) plasmid using the NdeI/XhoI sites.

2.5. Protein expression and purification

For the recombinant protein expression and purification, plasmids were transferred to expression host, E. coli BL21 (DE3) and plated on Luria-Bertani (LB) plates. A single colony from a

 doi:10.20944/preprints202306.2151.v1

fresh plate was picked and grown at 37°C in 3 mL of LB broth, containing 100 mg/mL ampicillin until OD_{600} = 0.6. They were inoculated in 100 mL of LB with ampicillin. Cells were grown at 37℃ with shaking until OD_{600} = 0.6. Cells were induced with 1 mM isopropyl-2-D-thiogalactopyranoside (IPTG) (GibcoBRL, NY) and grown for 4 h. Cells were then harvested by centrifugation at 6,000 g at 4℃ for 10 min. Harvested cells were resuspended in 50 mM Tris-HCl buffer (pH 8.0), and disrupted by sonication. The crude cell lysates were separated into total, soluble and insoluble fractions, which were analyzed by 10% SDS-PAGE. In order to purify the recombinant proteins, 10 mL of the crude cell lysates were loaded onto an IDA-miniexcellose affinity column (Keyprogen, Korea). The recombinant proteins were subsequently eluted with 5 mL of 0.5 M imidazole in the same buffer (50 mM phosphate, 0.5 N NaCl, pH 8.0). The purified proteins were then dialyzed against phosphate-buffered saline (PBS, pH 7.4) overnight at 4℃. The dialyzed proteins were further purified by size exclusion chromatography (SEC) using a Superdex G75 column (GE Healthcare, UT). The protein concentration was determined by Nano drop (Thermo scientific, MA). Finally, all recombinant proteins were concentrated to 1 mg/mL, and stored in -80℃ for further experiments.

2.6. Fluorescence measurement

The BiFC reporter protein and 6′-sialyllactose were utilized as components of the reporter system for the IAV assay. The mixture of 10 ug/mL reporter protein and 10 mM 6′-sialyllactose was incubated at 37°C for 1 h with various concentrations of IAV. The relative fluorescence intensity was measured as the fluorescence reconstitution using a Tecan Infinite 200 microplate reader (Tecan, Switzerland) at excitation/emission wavelengths of 513/530 nm (excitation/emission slit widths 5/5 nm). After background subtraction, the fluorescence signal was presented as mean ± SEM in the average relative fluorescence units (RFU). All fluorescence measurements reported here were repeated in a minimum of three independent experiments, and the results from three experiments were averaged.

3. Results and Discussion

3.1. Rationale

GGBP, a periplasmic binding protein found in bacteria, undergoes conformational changes upon binding to sugar ligands (i.e., galactose, glucose, lactose, etc.) [28–30]. This structural alteration has been previously utilized for identification of galactose and glucose ligand binding by introducing fluorescent tags into GGBP [31,32]. When integrated with the BiFC system, the unique hinge-twist motion of GGBP can be harnessed for biosensing applications. Herein, we aimed to develop an IAV sensing system designed by combining GGBP with the BiFC reporter protein. Figure 1 shows schematic diagram of in vitro detection of IAV using GGBP-based BiFC reporter system. Briefly, the NA activity of IAV cleaves the sialic acid moiety from 6'-sialyllactose, releasing lactose in a free state. Upon binding of the released lactose to the binding site between two lobes of GGBP, the proximity between the lobes is induced by hydrogen bonding between the lobe and the sugar ligand, resulting in a closed configuration. In our study, we employed the EYFP fluorescence complementation system, initially developed by Hu et al. [33] in 2002. Fluorescence reconstitution occurs due to ligand-induced structural changes in GGBP, and the fluorescence intensity directly correlates with the concentration of IAV, allowing for quantitative measurement.

Preprints (www.preprints.org) | NOT PEER-REVIEWED | Posted: 29 June 2023 doi:10.20944/preprints202306.2151.v1

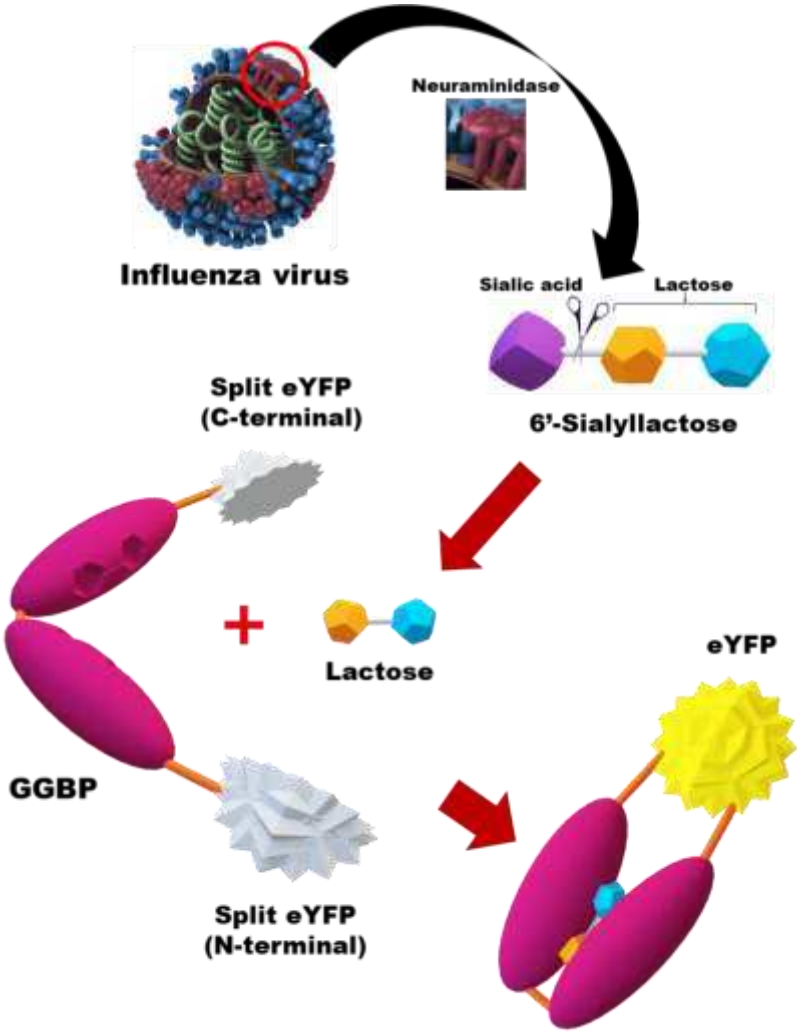

Figure 1. Schematic diagram of in vitro detection of IAV (H1N1) using the GGBP-based BiFC reporter system. When the NA of IAV cleaves the sialic acid residues of 6'-sialyllactose, lactose is released. Upon binding of the released lactose to the binding pocket between the two lobes of GGBP, structural changes in GGBP are induced, leading to the reconstitution of split eYFP fragments.

3.2. Characterization of the GGBP-based BiFC reporter system

Figure 2A shows construction of the GGBP-based BiFC reporter system. Based on previous studies on the split positions of eYFP, two types of the reporter variants were generated, YN1YC155 harboring the split between the seventh and eighth β-strands (the cut site between residues 154 and 155) [33,34] and YN1YC173 harboring the split between the eighth and ninth β-strands (the cut site between residues 172 and 173) [35,36] of eYFP. The two non-fluorescent fragments of eYFP were located at the N-terminus of GGBP and the loop region between residues 32 and 33 of GGBP, without incorporating any amino acid residues that contribute to ligand recognition, as previously reported [28]. The construction and purification of the reporter proteins were described in detail in the Materials and Methods section. After IPTG induction, there was an obvious band around the molecular weight of 63.8 kDa, which is consistent with the expected molecular weight of the recombinant reporter proteins (Figure 2B), and the YN1YC173 reporter protein profiles of the different fractions from the purification are shown in Figure 2C.

Preprints (www.preprints.org) | NOT PEER-REVIEWED | Posted: 29 June 2023 doi:10.20944/preprints202306.2151.v1

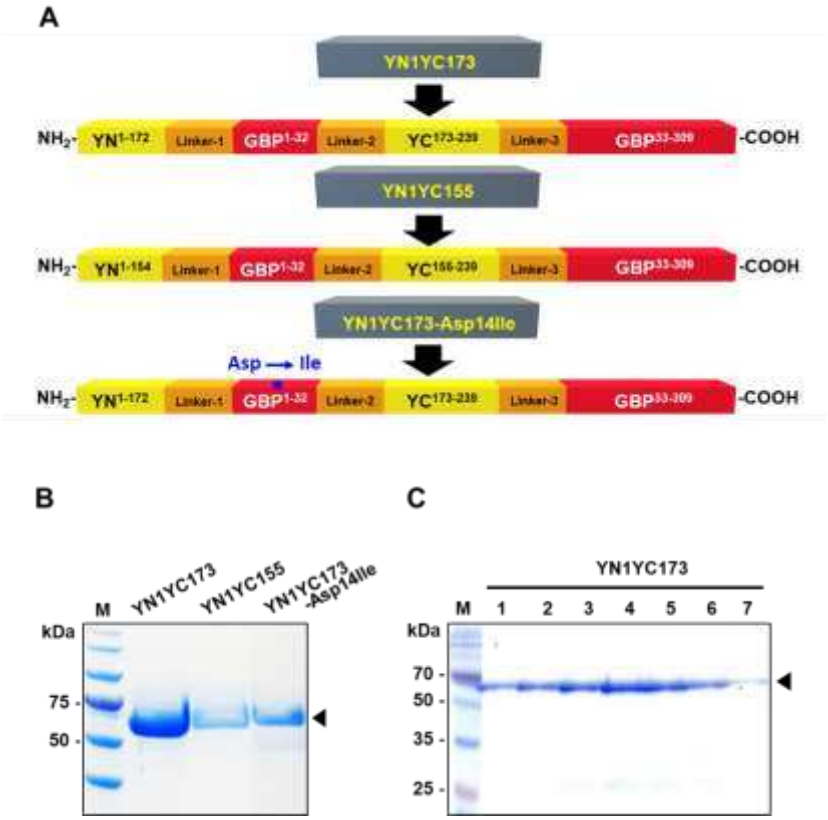

Figure 2. Construction, expression and purification of the reporter proteins. (A) Construction of the GGBP-based BiFC reporters. The YN1YC173 and YN1YC155 reporters comprise 4 domains of YN1-172-linker-1, GGBP1-32-linker-2, YC173-239-linker-3 and GGBP33-309, and YN1-154-linker-1, GGBP1-32-linker-2, YC155-239-linker-3 and GGBP33-309, respectively. The YN1YC173-Asp14Ile reporter is a mutant construct of YN1YC173, in which Asp-14 (*) of GGBP is substituted with an aliphatic residue (Ile). Linker-1, GTSSHM; Linker-2, GTGSGS; Linker-3, GSGHM. (B) SDS-PAGE analysis of the recombinant GGBP-based BiFC reporters (YN1YC173, YN1YC155 and YN1YC173-Asp14Ile. After IPTG induction, purified reporter proteins were then analyzed on 10% SDS–PAGE gel. Lane 1, protein marker; Lane 2, YN1YC173; Lane 3, YN1YC155; Lane 4, YN1YC173-Asp14Ile. (C) Analysis of the protein-containing fractions with SDS-PAGE. The numbers in the lanes correspond to the fractions of the eluted YN1YC173 reporter protein. The arrowhead indicates the expressed 63.8-kDa reporter proteins.

Figure 3 illustrates the comparison of fluorescence intensity enhancements in response to a sugar ligand (i.e., galactose), between the two reporters. The average relative fluorescence units (RFU) in the YN1YC155 reporter were observed to be relatively lower than those in the YN1YC173 reporter, approximately 80% compared to the YN1YC173 reporter. Based on the responses of the reporter proteins to the sugar ligand, it was concluded that among the two available reporters, the YN1YC173 reporter is more suitable as an IAV sensor. Therefore, we decided to utilize the YN1YC173 reporter for further experiments in IAV detection.

Asp-14 in GGBP is situated at the ligand-binding site and forms hydrogen bonds with the hydroxyl epimers at position 4 of glucose and galactose [37]. Therefore, substituting Asp with an alternative residue was anticipated to alter the specificity of GGBP. To examine this, a mutant BiFC reporter YN1YC173-Asp14Ile was prepared through site-directed mutagenesis of GGBP, where Asp-14 was replaced with an aliphatic residue (Ile). As shown in Figure 3, the fluorescence recovery of the mutant reporter was observed at a level of 24% compared to that of the wild reporter (YN1YC173) in response to the sugar ligand. Given that the increase in fluorescence intensity of the reporter reflects conformational changes of GGBP in the presence of its cognate ligand, this result suggests that although the sugar ligand has the ability to bind to the wild reporter, its ability to bind to the mutant reporter is limited, which aligns well with the observations reported by Sakaguchi-Mikami et al.,

Preprints (www.preprints.org) | NOT PEER-REVIEWED | Posted: 29 June 2023 doi:10.20944/preprints202306.2151.v1

stating that the Kd value of the mutant GGBP (Asp14Ile) for galactose was calculated to be 35 uM, whereas that of the wild GGBP to be 0.25 uM, thereby indicating that the mutant GGBP (Asp14Ile) lost its galactose-binding ability [37]. It is noteworthy that in the absence of galactose, the average RFU in the wild reporter sample was almost negligible, whereas in the presence of galactose, it was significantly lower compared to that in the mutant reporter samples. This may imply that the design of the IAV-sensing reporter incorporates a structure that prevents the unintended self-assembly of split eYFP fragments in the absence of a sugar ligand.

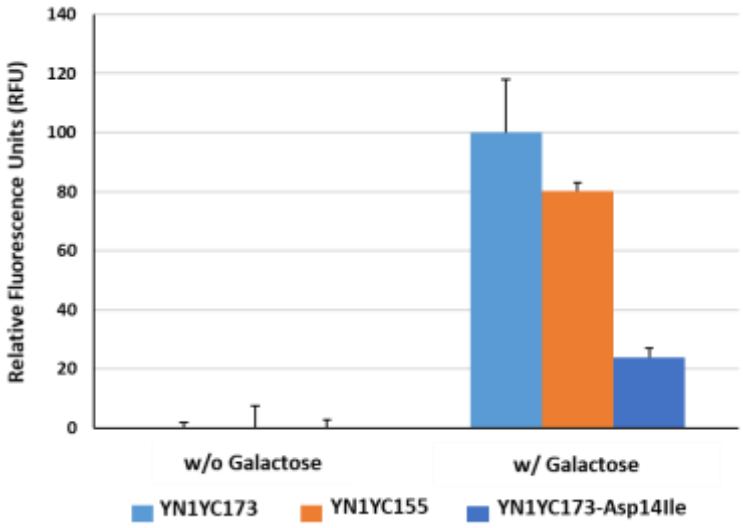

Figure 3. Functional evaluation of the GGBP-based BiFC reporter system. The fluorescence reconstitution in response to a sugar ligand was compared among YN1YC173, YN1YC155 and YN1YC173-Asp14Ile.

NA serves as a potential enzymatic marker for rapid viral diagnosis. Recently, an intriguing study on the detection of IAV through the enzymatic activity of NA using a nanopore sensor has been reported [38]. In that study, 6′-sialylgalactose was employed as a substrate for viral NA, and the structural changes of GGBP, induced by galactose cleaved from 6′-sialylgalactose, were measured using a Cytolysin A-based nanopore sensor. Generally, in GGBP-based IAV sensors targeting NA, either 6′-sialylgalactose or 6′-sialylglucose can be used as substrates for NA. From an economic point of view, choosing 6′-sialyllactose as a substrate that interacts with NA can be beneficial due to its cost-effectiveness. Since it is a naturally occurring oligosaccharide abundant in mammalian milk, indicating that it can be sourced from a readily available and abundant resource. Therefore, to explore the potential use of 6′-sialyllactose as a substrate for the BiFC-based IAV sensor, we compared the fluorescence reconstitutions of the reporter in response to glucose (10 mM), galactose (10 mM) and lactose. As shown in Figure 4A, comparing to the fluorescence intensity of the reporter without any ligand, three all ligands clearly induced fluorescence restoration with similar fluorescence enhancements under our experimental settings. These findings are in good agreement with the results reported by Taneoka et al., stating that GGBP exhibits similar levels of reactivity with not only glucose and galactose, but also lactose [28]. Next, to verify whether the fluorescence recovery of the BiFC reporter was due to specific interaction with lactose, we measured the changes in fluorescence complementation of the BiFC reporter in response to lactose concentrations ranging from 1 uM to 10 mM. As shown in Figure 4B, the BiFC reporter exhibited fluorescence intensity enhancements with increasing lactose concentration, displaying a high degree of regression analysis fit with a high R-squared value ($R^2 = 0.9376$, $p < 0.01$), thereby indicating that lactose has the ability to induce conformational alterations in the reporter protein.

Preprints (www.preprints.org) | NOT PEER-REVIEWED | Posted: 29 June 2023 doi:10.20944/preprints202306.2151.v1

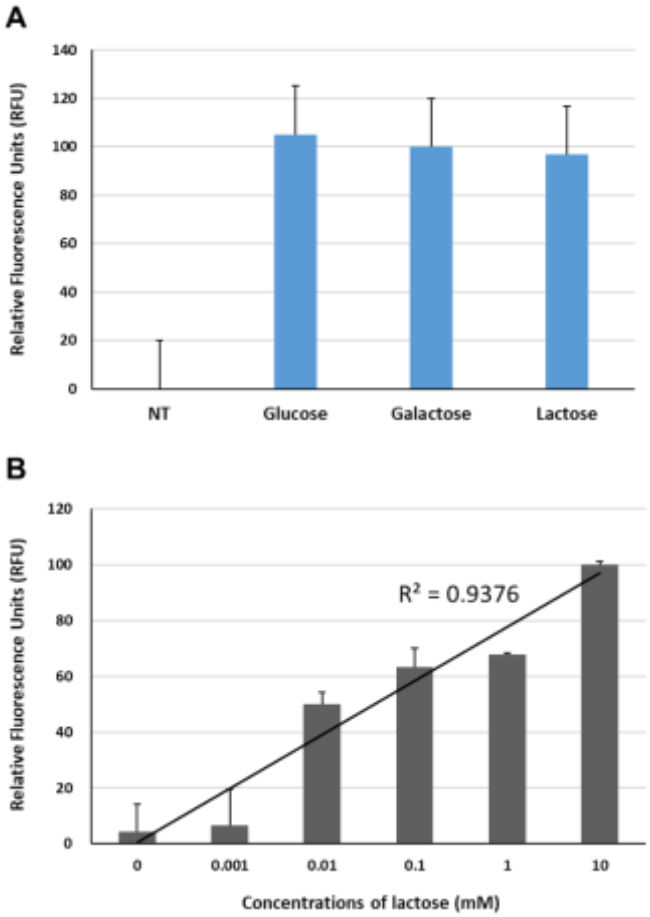

Figure 4. Measurement of fluorescence complementation of YN1YC173 (A) in response to glucose (10 mM), galactose (10 mM) and lactose (10 mM), and (B) under various concentrations of lactose. NT, non-treatment.

3.3. Functional evaluation for IAV detection

To assess the efficacy of our reporter system for the detection of IAV (H1N1), we investigated whether lactose was released freely from 6′-sialyllactose substrate in response to IAV, subsequently inducing fluorescence reconstitution. The BiFC response of the reporter protein was analyzed upon treatment with lactose (10 mM), 6′-sialyllactose (10 mM) only and 6′-sialyllactose with H1N1 (4×10^3 $TCID_{50}$/mL). Additionally, the influence of oseltamivir (10 uM), an inhibitor of NA, on the fluorescence recovery changes was investigated for each sample. As shown in Figure 5, an increase in fluorescence intensity was observed in reporter samples treated with lactose, while oseltamivir did not affect the fluorescence signal. In reporter samples treated with 6′-sialyllactose only, the fluorescence restoration decreased to approximately 20% of that observed in lactose-treated reporter regardless of oseltamivir treatment, indicating that the fluorescence reconstitution does not occur unless lactose is freely released by cleavage of sialic acid residues from 6′-sialyllactose. However, in samples containing both 6′-sialyllactose and H1N1, approximately 85% efficiency of fluorescence recovery was observed in the absence of oseltamivir, whereas the presence of oseltamivir led to a decrease in fluorescence intensity by nearly half the level of it. This can be interpreted as the inhibitory effect of oseltamivir on the NA activity of H1N1, which hinders the detachment of lactose from 6′-sialyllactose, thus preventing the structural changes in GGBP and resulting in inhibition of the fluorescence reconstitution.

Preprints (www.preprints.org) | NOT PEER-REVIEWED | Posted: 29 June 2023 doi:10.20944/preprints202306.2151.v1

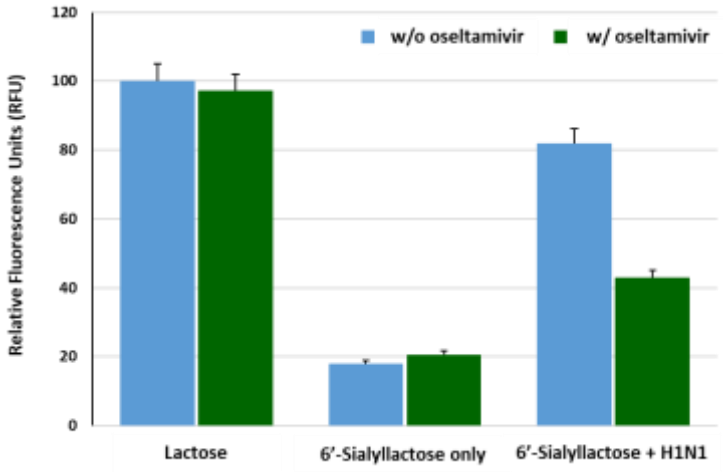

Figure 5. Functional evaluation of the GGBP-BiFC-based IAV sensor. The fluorescence intensity enhancements of the reporter (10 ug/mL) were analyzed in response to lactose (10 mM), 6′-sialyllactose (10 mM) only and 6′-sialyllactose treated with H1N1 (4 x 10^3 $TCID_{50}$/mL). To examine the reliability of the H1N1 detection system, the inhibitory effect of the oseltamivir (10 uM) on NA activity was tested.

3.4. Sensitivity for IAV detection

We examined the IAV (H1N1) concentration-dependent fluorescence reconstitutions from the BiFC reporter. The H1N1 samples were prepared at concentration ranging from 1 x 10^0 $TCID_{50}$/mL to 1 x 10^7 $TCID_{50}$/mL by 1/10 serial dilution, under conditions of 10 ug/mL reporter protein and 10 mM 6′-sialyllactose. The 6′-sialyllactose sample in the absence of virus (NT, non-treatment) was prepared as a control. The fluorescence intensity in response to 10 mM lactose was set as 100.0%, and the impact of virus concentration variations on fluorescence reconstitution was monitored. Virus amplification was performed by culturing MDCK cells in DMEM medium containing trypsin (1 ug/mL), followed by virus treatment and harvesting of samples after 3-5 days of cell destruction. The BiFC reporter protein, 6′-sialyllactose and H1N1 were placed in each single well of a 96-well plate and incubated at 37℃ for 1 h, allowing sufficient time for the viral NA to liberate sialic acid residues from 6′-sialyllactose and for the released lactose to induce structural changes in GGBP. Figure 6 shows the correlation between H1N1 concentration and fluorescence recovery. The average RFU gradually increased as the virus concentration increased, displaying a fitted line graph with a high R-squared value (R^2 = 0.973, $p < 0.01$). Our system exhibited a linear dependency within the range of from 1 x 10^0 $TCID_{50}$/mL to 1 x 10^7 $TCID_{50}$/mL, allowing for the quantitative measurement of H1N1. The estimated limit of detection (LOD) of this method was 4 x 10^1 $TCID_{50}$/mL, as the average RFU in the presence of H1N1 at 4 x 10^1 $TCID_{50}$/mL was observed to be approximately 46.875%, which was three times high compared to the control sample (approximately 15.625%). Narrow variations in fluorescence signals were also observed at each point of virus detection, which implies an increase in the reliable fluorescence signal due to the fluorescence reconstitution as a result of conformational changes in GGBP when lactose, binds to GGBP in the presence of H1N1. Typically, the viral concentration of respiratory viruses including IAV, found in droplets released into the air during the initial stages of coughing in infected individuals, is estimated to be approximately 1 x 10^3 $TCID_{50}$/mL. This means that a limit of detection should be lower than 1 x 10^3 $TCID_{50}$/mL to confirm the presence of infection in the early stages. Over the past decades, various detection techniques for IAV have been developed to enhance sensitivity. Previously reported PCR-based studies demonstrated a detection limit at the level of 1 x 10^2 $TCID_{50}$/mL [39–41]. Immunodiagnostic assays reported earlier showed a detection limit ranging from 1 x 10^3 to 1 x 10^4 $TCID_{50}$/mL [42–44]. Therefore, when comparing the sensitivity values to those previously reported, our BiFC reporter system exhibits a lower detection limit and a wider dynamic range. In on-site testing situations where direct detection without the need

Preprints (www.preprints.org) | NOT PEER-REVIEWED | Posted: 29 June 2023 doi:10.20944/preprints202306.2151.v1

for virus amplification is required, an ultra-high sensitive sensor is inevitable. In this regard, the achievement of 4 x 10^1 $TCID_{50}$/mL detection limit for H1N1 in the current study indicates that this method holds the potential for applicability in the field of primary screening, which requires high sensitivity direct detection.

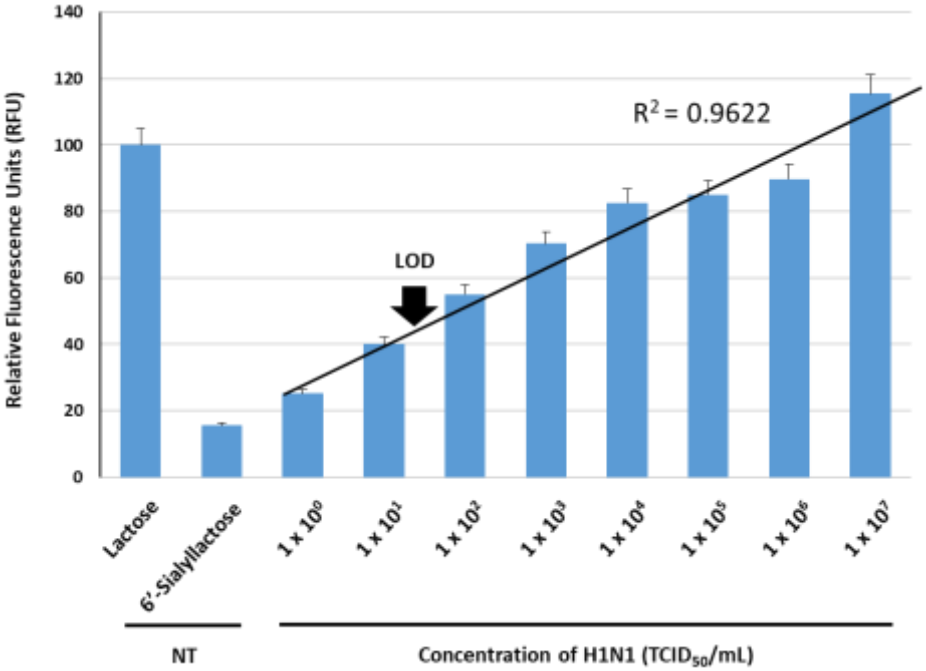

Figure 6. Sensitivity of the GGBP-based BiFC reporter system for IAV detection. The average RFU under various concentrations of H1N1 ranging from 1 x 10^0 $TCID_{50}$/mL to 1 x 10^7 $TCID_{50}$/mL were measured. NT, non-treatment.

3.5. Specificity for IAV detection

To evaluate the specificity of this approach, we investigated four different subtypes of IAV (H1N1, H1N2, H3N8 and H6N5) and four different respiratory viruses (RSV A, RSV B, adenovirus and rhinovirus). The concentration of all examined viruses was 1 x 10^7 $TCID_{50}$/mL. As shown in Figure 7, the average RFU induced by H1N1, H1N2, H3N8 and H6N5 were 115.2%, 127.5%, 114.7% and 110.9%, respectively, with the signal value for the lactose sample in the absence of virus (NT, non-treatment) set as 100.0%. Given that the current system relies on the activity of NA within IAV, it was easily predictable result. In contrast, the average RFU in response to other respiratory viruses such as RSV A, RSV B, adenovirus and rhinovirus were measured at 40.5%, 45.4%, 47.7% and 38.3%, respectively, exhibiting weak signals in the presence of these NA-deficient viruses, indicating the specificity of our system for IAV detection. Therefore, we expect that the GGBP-based BiFC reporter system will be useful for the specific detection of IAV.

Preprints (www.preprints.org) | NOT PEER-REVIEWED | Posted: 29 June 2023 doi:10.20944/preprints202306.2151.v1

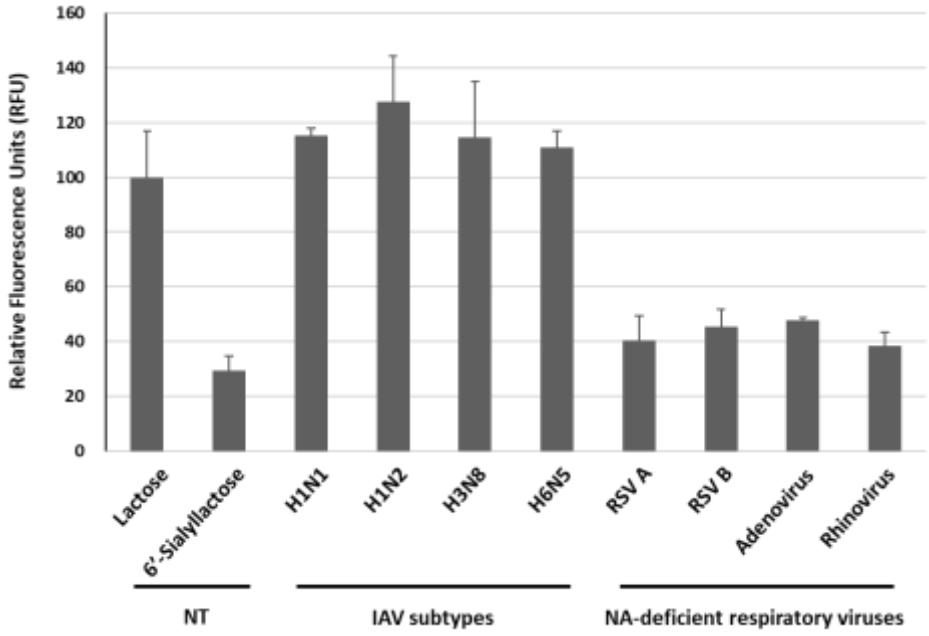

Figure 7. Specificity of the GGBP-based BiFC reporter system for IAV detection over other NA-deficient respiratory viruses such as RSV A, RSV B, adenovirus and rhinovirus. The concentration was 1 x 10^7 $TCID_{50}$/mL for all viruses examined. NT, non-treatment.

4. Conclusions

In summary, a facile, highly sensitive and specific IAV sensing system, designed by combining a GGBP with a BiFC reporter protein and 6'-sialyllactose as a substrate, was developed. The fluorescence reconstitution of the GGBP-based BiFC reporter is triggered by conformational changes in GGBP upon the binding of lactose, which is cleaved from 6'-silalyllactose by NA enzyme activity of IAV, to the GGBP. The BiFC reporter system enables the facile detection of IAV without the need for virus culture or RNA extraction processes. The current system demonstrated exceptional sensitivity for detecting IAV (H1N1) by exhibiting a linear dynamic range spanning from 1 x 10^0 $TCID_{50}$/mL to 1 x 10^7 $TCID_{50}$/mL, with a remarkable detection limit of 4 x 10^1 $TCID_{50}$/mL. The reporter system also exhibited weak fluorescence intensity enhancements in the presence of NA-deficient viruses, indicating the specificity of the system for IAV detection. In on-site testing where immediate virus detection without the requirement of virus amplification is crucial, the demand for an ultra-high sensitive sensor becomes imperative. In this context, our current study's attainment of a detection limit of 4 x 10^1 $TCID_{50}$/mL for H1N1 highlights the potential applicability of our system in the field of primary screening, where high sensitivity detection and large-scale sample monitoring are required.

Author Contributions: Conceptualization, U.J.L., Y.O. and M.K.; methodology, U.J.L. and Y.O.; validation, U.J.L., Y.O., O.S.K. and Y.B.S.; data analysis, U.J.L., Y.O., O.S.K. and Y.B.S.; resources, O.S.K. and Y.B.S.; software, O.S.K. and Y.B.S.; writing—original draft preparation, U.J.L. and Y.O.; writing—review and editing, M.K.; supervision, M.K.; funding acquisition, M.K. All authors have read and agreed to the published version of the manuscript.

Funding: This work was supported by the National Research Council of Science and Technology (NST) grant by the Korea Government (CRC22021-300), the Korea Research Institute of Bioscience and Biotechnology (KRIBB) Initiative Research Program (KGM9952314), and the Bio & Medical Technology Development Program of the National Research Foundation (NRF) funded by the Ministry of Science & ICT (2021M3A9I5021439).

Institutional Review Board Statement: Not applicable.

Informed Consent Statement: Not applicable.

Data Availability Statement: The data presented in this study are available on request from the corresponding author (M.K.).

Conflicts of Interest: The authors declare no conflict of interest.

References

1. Javanian, M.; Barary, M.; Ghebrehewet, S.; Koppolu, V.; Vasigala, V.; Ebrahimpour, S. A brief review of influenza virus infection. *J. Med. Virol.* **2021**, *93*, 4638–4646.
2. Krammer, F.; Smith, G.J.D.; Fouchier, R.A.M.; *et al.* Influenza. *Nat. Rev. Dis. Primers* **2018**, *4*, 3.
3. Babazadeh, A.; Afshar Z.M.; Javanian, M.; *et al.* Influenza vaccination and Guillain-Barré syndrome: reality or fear. *J. Transl. Int. Med.* **2019**, *7*, 137–142.
4. Hajjar S.A.; McIntosh K. The first influenza pandemic of the 21st century. *Ann. Saudi. Med.* **2010**, *30*, 1–10.
5. Kim, H.; Webster, R.G.; Webby, R.J. Influenza virus: dealing with a drifting and shifting pathogen. *Viral Immunol.* **2018**, *31*, 174–183.
6. Dou, D.; Revol, R.; Östbye, H.; Wang, H.; Daniels, R. Influenza A virus cell entry, replication, virion assembly and movement. *Front. Immunol.* **2018**, *9*, 1581.
7. Byrd-Leotis, L.; Cummings, R.D.; Steinhauer, D.A. The interplay between the host receptor and influenza virus hemagglutinin and neuraminidase. *Int. J. Mol. Sci.* **2017**, *18*, 1541.
8. Ravina; Manjeet; Mohan, H.; Narang, J. Pundir, S.; Pundir, C.S. A changing trend in diagnostic methods of Influenza A (H3N2) virus in human: a review. *3 Biotech.* **2021**, *11*, 87.
9. Liu, Y.; Zhao, J.; Peng, X.; Lu, G.; Shi, W.; Feng, Z.; Xu, H.; Cui, S.; Pan, Y.; Zhang, D.; Yang, P.; Wang, Q. Application of a ddRT-PCR to quantify seasonal influenza virus for viral isolation. *Biosafety and Health* **2022**, *4*, 299–302.
10. Woźniak-Kosek, A.; Kempińska-Mirosławska, B.; Hoser, G. Detection of the influenza virus yesterday and now. *Acta Biochim. Pol.* **2014**, *61*, 465–470.
11. Gavin, P.J.; Thomson, R.B. Review of rapid diagnostic tests for influenza. *Clin. Appl. Immunol. Rev.* **2004**, *4*, 151–172.
12. Nakaya, Y.; Shojima, T.; Hoshino, S.; Miyazawa, T. Focus assay on felix-dependent feline leukemia virus. *J. Vet. Med. Sci.* **2010**, *72*, 117–21.
13. Xue, J.; Chambers, B.S.; Hensley, S.E.; López, C.B. Propagation and characterization of influenza virus stocks that lack high levels of defective viral genomes and hemagglutinin mutations. *Front. Microbiol.* **2016**, *7*, 1–15.
14. Eisfeld, A.; Neumann, G.; Kawaoka, Y. Influenza A virus isolation, culture and identification. *Nat. Protoc.* **2014**, *9*, 2663–2681.
15. Nagy, A.; Černíková, L.; Kunteová, K.; Dirbáková, Z.; Thomas, S.S.; Slomka, M.J.; *et al.* A universal RT-qPCR assay for "One Health" detection of influenza A viruses. *PLoS ONE* **2021**, *16*, e0244669.
16. Yang, F.; Xu, L.; Liu, F.; *et al.* Development and evaluation of a TaqMan MGB RT-PCR assay for detection of H5 and N8 subtype influenza virus. *BMC Infect. Dis.* **2020**, *20*, 550.
17. Wang, J.; Tai, W.; Angione, S.L.; John, A.R.; Opal, S.M.; Artenstein, A.W.; Tripathi, A. Subtyping clinical specimens of influenza A virus by use of a simple method to amplify RNA targets. *J. Clin. Microbiol.* **2013**, *51*, 3324–3330.
18. Thi, V.L.D.; Herbst, K.; Boerner, K.; Meurer, M.; Kremer, L.P.; Kirrmaier, D.; Freistaedter, A.; Papagiannidis, D.; Galmozzi, C.; Boulant, S.; *et al.* A colorimetric RT-LAMP assay and LAMP-sequencing for detecting SARS-CoV-2 RNA in clinical samples. *Sci. Transl. Med.* **2020**, *12*, 7075.
19. Leirs, K.; Tewari, K.P.; Decrop, D.; Pérez-Ruiz, E.; Leblebici, P.; Van Kelst, B.; Compernolle, G.; Meeuws, H.; Van Wesenbeeck, L.; Lagatie, O.; Stuyver, L. Bioassay development for ultrasensitive detection of influenza a nucleoprotein using digital ELISA. *Anal. Chem.* **2016**, *88*, 8450–8458.
20. Dziąbowska, K.; Czaczyk, E.; Nidzworski, D. Detection methods of human and animal influenza virus—Current trends. *Biosensors* **2018**, *8*, 94.
21. Lin, X.; Liu, X.Y.; Zhang, B.; *et al.* A rapid influenza diagnostic test based on detection of viral neuraminidase activity. *Sci. Rep.* **2022**, *12*, 505.
22. Vemula, S.V.; Zhao, J.; Liu, J.; Wang, X.; Biswas, S.; Hewlett, I. Current approaches for diagnosis of influenza virus infections in humans. *Viruses* **2016**, *8*, 96.
23. Romei, M.G.; Boxer, S.G. Split green fluorescent proteins: scope, limitations, and outlook. *Annu. Rev. Biophys.* **2019**, *48*, 19–44.

24. Kodama, Y.; Hu, C.D. Bimolecular fluorescence complementation (BiFC): a 5-year update and future perspectives. *Biotechniques* **2012**, *53*, 285–298.
25. Kerppola, T.K. Visualization of molecular interactions using bimolecular fluorescence complementation analysis: characteristics of protein fragment complementation. *Chem. Soc. Rev.* **2009**, *38*, 2876–2886.
26. Velay, F.; Soula, M.; Mehrez, M.; *et al.* MoBiFC: development of a modular bimolecular fluorescence complementation toolkit for the analysis of chloroplast protein–protein interactions. *Plant Methods* **2022**, *18*, 69.
27. Jeong, J.; Kim, S.K.; Ahn, J.; Park, K.; Jeong, E.J.; Kim, M.; Chung, B.H. Monitoring of conformational change in maltose binding protein using split green fluorescent protein. *Biochem. Biophys. Res. Commun.* **2006**, *339*, 647–651.
28. Taneoka, A.; Sakaguchi-Mikami, A.; Yamazaki, T.; Tsugawa, W.; Sode, K. The construction of a glucose-sensing luciferase. *Biosens. Bioelectron.* **2009**, *25*, 76–81.
29. Unione, L.; Ortega, G.; Mallagaray, A.; Corzana, F.; Perez-Castells, J.; Canales, A.; Jimenez-Barbero, J.; Millet, O. Unraveling the conformational landscape of ligand binding to glucose/galactose-binding protein by paramagnetic NMR and MD simulations. *ACS Chem. Biol.* **2016**, *11*, 2149–57.
30. Borrok, M.J.; Kiessling, L.L.; Forest, K.T. Conformational changes of glucose/galactose-binding protein illuminated by open, unliganded, and ultra-high-resolution ligand-bound structures. *Protein Sci.* **2007**, *16*, 1032–41.
31. Salins, L.L; Ware, R.A.; Ensor, C.M.; Daunert, S. A novel reagentless sensing system for measuring glucose based on the galactose/glucose-binding protein. *Anal. Biochem.* **2001**, *294*, 19–26.
32. Zukin, R.S.; Strange, P.G.; Heavey, R.; Koshland, D.E. Properties of the galactose binding protein of Salmonella typhimurium and *Escherichia coli*. *Biochemistry* **1977**, *16*, 381–386.
33. Hu, C.D.; Chinenov, Y.; Kerppola, T.K. Visualization of interactions among bZIP and Rel family proteins in living cells using bimolecular fluorescence complementation. *Mol. Cell* **2002**, *9*, 789–798.
34. Walter, M.; Chaban, C.; Schütze, K.; Batistic, O.; Weckermann, K.; Näke, C.; Blazevic, D.; Grefen, C.; Schumacher, K.; Oecking, C.; Harter, K.; Kudla, J. Visualization of protein interactions in living plant cells using bimolecular fluorescence complementation. *Plant J.* **2004**, *40*, 428–438.
35. Hu, C.D.; Kerppola, T.K. Simultaneous visualization of multiple protein interactions in living cells using multicolor fluorescence complementation analysis. *Nat. Biotechnol.* **2003**, *21*, 539–545.
36. Waadt, R.; Schmidt, L.K.; Lohse, M.; Hashimoto, K.; Bock, R.; Kudla, J. Multicolor bimolecular fluorescence complementation reveals simultaneous formation of alternative CBL/CIPK complexes in planta. *Plant J.* **2008**, *56*, 505–516.
37. Sakaguchi-Mikami, A.; Taneoka, A.; Yamoto, R.; *et al.* Engineering of ligand specificity of periplasmic binding protein for glucose sensing. *Biotechnol. Lett.* **2008**, *30*, 1453–1460.
38. Kwak, D.K.; Kim, J.S.; Lee, M.K.; Ryu, K.S.; Chi, S.W. Probing the neuraminidase activity of influenza virus using a Cytolysin A protein nanopore. *Anal. Chem.* **2020**, *92*, 21, 14303–14308.
39. Hindiyeh, M.; Kolet, L.; Meningher, T.; Weil, M.; Mendelson, E.; Mandelboim, M. Evaluation of Simplexa Flu A/B & RSV for direct detection of influenza viruses (A and B) and respiratory syncytial virus in patient clinical samples. *J. Clin. Microbiol.* **2013**, *51*, 2421–2424.
40. Sambol, A.R.; Iwen, P.C.; Pieretti, M.; Basu, S.; Levi, M.H.; Gilonske, K.D.; Moses, K.D.; Marola, J.L.; Ramamoorthy, P. Validation of the Cepheid Xpert Flu A real time RT-PCR detection panel for emergency use authorization. *J. Clin. Virol.* **2010**, *48*, 234–238.
41. Gharabaghi, F.; Tellier, R.; Cheung, R.; Collins, C.; Broukhanski, G.; Drews, S.J.; Richardson, S.E. Comparison of a commercial qualitative real-time RT-PCR kit with direct immunofluorescence assay (DFA) and cell culture for detection of influenza A and B in children. *J. Clin. Virol.* **2008**, *42*, 190–193.
42. Landry, M.L.; Cohen, S.; Ferguson, D. Comparison of Binax NOW and Directigen for rapid detection of influenza A and B. *J. Clin. Virol.* **2004**, *31*, 113–115.
43. Ruest, A.; Michaud, S.; Deslandes, S.; Frost, E.H. Comparison of the Directigen flu A+B test, the QuickVue influenza test, and clinical case definition to viral culture and reverse transcription-PCR for rapid diagnosis of influenza virus infection. *J. Clin. Microbiol.* **2003**, *41*, 3487–3493.
44. Quach, C.; Newby, D.; Daoust, G.; Rubin, E.; McDonald, J. QuickVue influenza test for rapid detection of influenza A and B viruses in a pediatric population. *Clin. Diagn. Lab. Immunol.* **2002**, *9*, 925–926.

disclaim responsibility for any injury to people or property resulting from any ideas, methods, instructions or products referred to in the content.